JACS
JOURNAL OF THE AMERICAN CHEMICAL SOCIETY
Communication
pubs.acs.org/JACS

A Super-Reduced Diferrous [2Fe−2S] Cluster

Antonia Albers,[†] Serhiy Demeshko,[†] Kevin Pröpper,[†] Sebastian Dechert,[†] Eckhard Bill,[‡] and Franc Meyer*,[†]

[†]Institute of Inorganic Chemistry, Georg-August-University Göttingen, Tammannstrasse 4, D-37077 Göttingen, Germany
[‡]Max-Planck-Institute for Chemical Energy Conversion, Stiftstrasse 34 − 36, D-45470 Mülheim an der Ruhr, Germany

Supporting Information

ABSTRACT: A biomimetic [2Fe−2S] cluster has been isolated in the fully reduced diferrous form and characterized by X-ray diffraction. This completes a consistent series of synthetic analogues of protein-bound $[2Fe{-}2S]^{z}$ redox centers (z = 2+, 1+, 0) with identical capping ligands. ^{57}Fe Mössbauer data of the extremely oxidation-sensitive complex compare well with those of the very few reports of all-ferrous ferredoxins and Rieske centers; they confirm the $S_T = 0$ ground state and establish a lower limit for the exchange coupling, $-J \geq 30$ cm^{-1}.

Protein-bound iron−sulfur clusters are ubiquitous and multipurpose biological cofactors,[1] with cubane-type [4Fe−4S] and rhombic [2Fe−2S] clusters being the most common structural motifs. Their primary function is one-electron transfer, where the Fe/S core usually shuttles between two oxidation states.[2] For [4Fe−4S] clusters, the $[4Fe{-}4S]^{1+/2+}$ redox couple is most frequently encountered, while the $[4Fe{-}4S]^{2+/3+}$ couple is operative in so-called high-potential iron−sulfur proteins.[3] In contrast, [2Fe−2S] cofactors attain under physiological conditions only the $[2Fe{-}2S]^{1+/2+}$ redox couple. Mössbauer and NMR spectroscopy have shown that the metal ions are in the valence-localized oxidation states $Fe^{II}Fe^{III}$ in the reduced (1+) form and $Fe^{III}Fe^{III}$ in the oxidized (2+) form. Synthetic analogues for Fe/S clusters in general have significantly contributed to understanding their electronic structures.[4] However, only recently we succeeded for the first time in isolating and fully characterizing, including single crystal X-ray diffraction, a [2Fe−2S] model complex in its mixed-valent (1+) state, stabilized by two bis(benzimidazolato) capping ligands (Figure 1).[5,6] Now, we present the corresponding diferrous complex in the (0+) state, thus completing a consistent series of $[2Fe{-}2S]^{z}$ redox centers (z = 2+, 1+, 0) with identical terminal ligands.

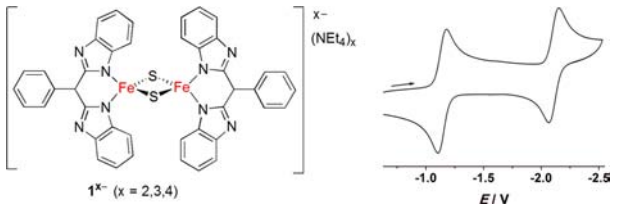

Figure 1. (Left) [2Fe−2S] clusters discussed in this work; (right) cyclic voltammogram of $\mathbf{1}^{2-}$ in MeCN at a scan rate of 100 mV/s; potentials are given in volts vs the Fc/Fc^{+} couple (Fc, ferrocen).

A tetranuclear all-ferrous $[4Fe{-}4S]^{0}$ cluster has been implicated for the unique Fe protein of nitrogenase in its fully reduced state and for one other protein,[7,8] and its emulation in small molecule models has been accomplished in recent years using either cyanide or N-heterocyclic carbenes as terminal ligands for the $[4Fe{-}4S]^{0}$ cubane.[9,10] Little is yet known about diferrous $[2Fe{-}2S]^{0}$ clusters. The all-ferrous forms of spinach and parsley ferredoxin have been produced by treatment of their oxidized forms, Fd_{ox}, with strong Cr^{II} reductants; it has been proposed that the Cr^{III} product from the first reduction remains bound to the ferredoxins and causes an upward shift of the redox potential that allows for the second reduction to occur.[11] The diferrous state has mainly been supported by Mössbauer evidence, showing a quadrupole doublet with δ = 0.71 mm/s and ΔE_Q = 2.75 mm/s at 4.2 K.[12] In Rieske clusters, redox potential leveling is achieved by coupling proton and electron transfer, and hence, the all-ferrous form with neutral histidine ligands could be produced electrochemically and characterized by UV−vis and Mössbauer spectroscopies (δ = 0.70 mm/s and ΔE_Q = 2.76 mm/s for the cysteine-ligated iron; δ = 0.81 mm/s and ΔE_Q = 2.32 mm/s for the histidine-ligated iron; at 4.2 K).[13] Given the difficulties in isolating even mixed-valent synthetic $[2Fe{-}2S]^{1+}$ analogues and their extremely low reduction potentials, it deemed unlikely that a fully reduced synthetic $[2Fe{-}2S]^{0}$ species could ever be isolated in substance.[4]

Bidentate bis(benzimidazolato) ligands have previously been shown to stabilize [2Fe−2S] clusters in their reduced states,[14] and the particular ligand with a backbone phenyl substituent (which also improves solubility and crystallization behavior) allowed for the first crystallographic characterization of a mixed-valent $[2Fe{-}2S]^{1+}$ complex $\mathbf{1}^{3-}$ (Figure 1).[5] The cyclic voltammogram of $\mathbf{1}^{2-}$ was unusually well behaved and showed two reversible one-electron reduction processes at $E_{1/2}$ = −1.14 and −2.10 V versus Fc/Fc^{+} (corresponding to the $[2Fe{-}2S]^{1+/2+}$ and $[2Fe{-}2S]^{0/1+}$ couples), with a very large comproportionation constant of the mixed-valent species (K_c = 1.7 × 10^{16}). These characteristics suggested that further reduction might indeed be feasible for this system.

The electrochemical reduction of $\mathbf{1}^{3-}$ (c = 4.8 × 10^{-4} M) in DMF with 0.1 M $[NEt_4]BF_4$ at a potential of −2.40 V and at −15 °C was followed by UV−vis spectroscopy until no further

Received: November 26, 2012
Published: January 15, 2013

   dx.doi.org/10.1021/ja311563y | J. Am. Chem. Soc. 2013, 135, 1704−1707

changes were noticeable (Figure 2, left). Clean conversion to $\mathbf{1}^{4-}$ with three isosbestic points at 328, 402, and 442 nm was

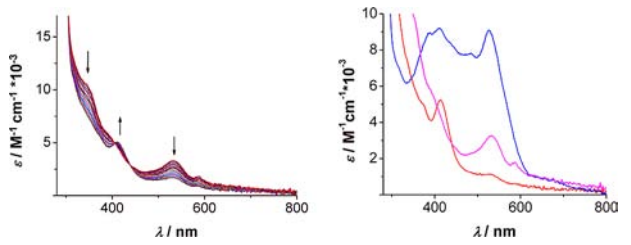

Figure 2. (Left) UV–vis spectra during constant potential coulometry recorded at −15 °C, −2.40 V vs Fc/Fc^+, $c = 4.8 \times 10^{-4}$ M, in DMF/0.1 M $[NEt_4]BF_4$; (right) overlay of the spectra of $\mathbf{1}^{2-}$ (blue), $\mathbf{1}^{3-}$ (magenta), and $\mathbf{1}^{4-}$ (red) in DMF solution.

observed. The intensity of the band for $\mathbf{1}^{3-}$ at 530 nm decreases to ε = 1150 M^{-1} cm^{-1} and the shoulder at 586 nm largely vanishes to ε = 630 M^{-1} cm^{-1}, while a new band for $\mathbf{1}^{4-}$ rises at 413 nm (ε = 5200 M^{-1} cm^{-1}). Overall, the intensity of the spectrum decreases continuously upon going from diferric $\mathbf{1}^{2-}$ to mixed-valent $\mathbf{1}^{3-}$ and further to $\mathbf{1}^{4-}$ ($\mathbf{1}^{2-}$ is dark red, $\mathbf{1}^{3-}$ is magenta, while $\mathbf{1}^{4-}$ is orange; Figure 2 right). This bleaching is reminiscent of the spectral changes seen for the Rieske protein upon reduction.[13] Shifting the potential back to −1.6 V leads to complete reoxidation of $\mathbf{1}^{4-}$ to mixed-valent $\mathbf{1}^{3-}$.

The all-ferrous cluster $\mathbf{1}^{4-}$ was then synthesized chemically by addition of potassium anthracene to a DMF solution of $(NEt_4)_2\mathbf{1}$ and precipitation of crude $K_2(NEt_4)_2\mathbf{1}$ with an excess of diethyl ether. Crystals of the sought-after $(NEt_4)_4\mathbf{1}$ salt could be obtained, after addition of $(NEt_4)Br$, by slow diffusion of diethyl ether into a DMF solution at 4 °C. Fully reduced $\mathbf{1}^{4-}$ is extremely sensitive toward oxidants and has a very high tendency to revert back to $\mathbf{1}^{3-}$; it thus is best handled and stored in the presence of excess potassium anthracene reductant.

The molecular structure of the anion of $(NEt_4)_4\mathbf{1}$ is shown in Figure 3, together with an overlay of the central $[2Fe–2S]^z$

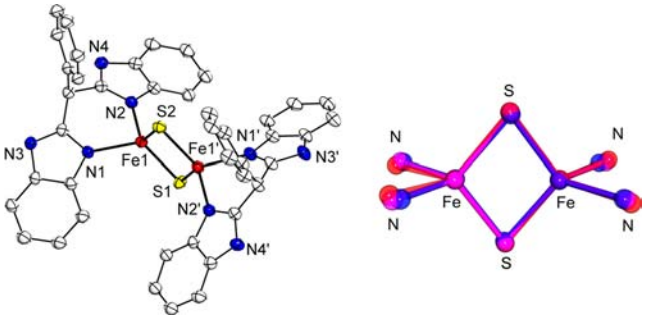

Figure 3. (Left) ORTEP plot of the molecular structure of $\mathbf{1}^{4-}$ (thermal ellipsoids set at 30% probability). For clarity, all hydrogen atoms are omitted (symmetry operation used to generate equivalent atoms: (′) 1 − x, y, 0.5 − z); (right) overlay of the $\{Fe_2S_2\}$ cores of $\mathbf{1}^{2-}$ (blue), $\mathbf{1}^{3-}$ (magenta), and $\mathbf{1}^{4-}$ (red).

cores of $\mathbf{1}^{2-}$, $\mathbf{1}^{3-}$ and $\mathbf{1}^{4-}$. Since mixed-valent $\mathbf{1}^{3-}$ was previously characterized with different cations,[5] its $[NEt_4]^+$ salt was now prepared and analyzed by X-ray diffraction (see Supporting Information (SI)). This gives rise to the unique situation that structural information is available for the complete series of [2Fe–2S] model complexes $\mathbf{1}(NEt_4)_x$ (x = 2, 3, 4) with the same bis(benzimidazolato) capping ligands and the same type of cation, allowing us to asses the effect of sequential reduction on the core structures.[15] Upon going from diferric $\mathbf{1}^{2-}$ to mixed-valent $\mathbf{1}^{3-}$ and further to $\mathbf{1}^{4-}$, the $\{Fe_2S_2\}$ rhomb undergoes a slight but continuous expansion: $d_{Fe\cdots Fe}$ rises from around 2.70 to 2.73 Å and further to 2.75 Å, and Fe–S bonds lengthen from 2.19/2.21 to 2.23/2.24 and further to 2.26/2.27 Å (Table 1). A similar elongation is observed for the Fe–N

Table 1. Selected Atom Distances (Å) and Bond Angles (deg) for $\mathbf{1}^{2-}$, $\mathbf{1}^{3-}$, and $\mathbf{1}^{4-}$

	$\mathbf{1}^{2-}$	$\mathbf{1}^{3-}$	$\mathbf{1}^{4-}$
d(Fe···Fe)	2.70	2.73	2.75
d(Fe–S)	2.19/2.21	2.23/2.24	2.26/2.27
d(Fe–N)	1.98/1.99	2.06/2.07	2.11/2.12
∠(N–Fe–N)	92.84	88.18	84.35
∠(S–Fe–S)	104.27	104.84	105.19

bonds to the terminal bis(benzimidazolato) ligands, and the N–Fe–N angles become increasingly acute.[5] However, as is evident from the overlay in Figure 3, the global structural changes around the tetrahedrally coordinated iron atoms are relatively small upon sequential injection of two electrons into the cluster core. This reflects the low reorganization associated with redox changes of the $\{Fe_2S_2\}$ rhomb, which makes these [2Fe–2S] clusters preferred electron transfer sites in nature.

The Mössbauer spectrum of solid $(NEt_4)_4\mathbf{1}$ at 6 K shows one quadrupole doublet with δ = 0.79 mm/s and ΔE_Q = 2.67 mm/s clearly indicating the presence of high spin Fe^{II} (Figure 4). The

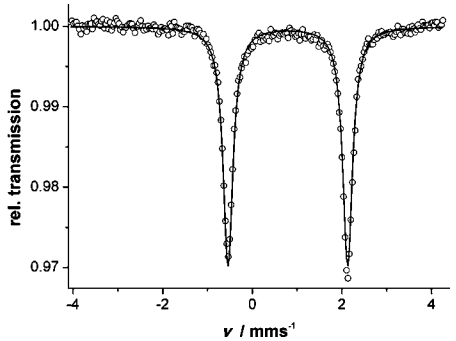

Figure 4. Zero field Mössbauer spectrum of solid $(NEt_4)_4\mathbf{1}$ at 6 K. The line represents a fit with δ = 0.79 mm/s and ΔE_Q = 2.67 mm/s.

parameters are in excellent agreement with those found for the all-ferrous forms of a [2Fe–2S] ferredoxin (δ = 0.71 mm/s, ΔE_Q = 2.75 mm/s; see above)[12] as well as for the super-reduced Rieske protein at 4.2 K (δ = 0.70 mm/s, ΔE_Q = 2.76 mm/s for the $\{FeS_2Cys_2\}$ site and δ = 0.81 mm/s, ΔE_Q = 2.32 mm/s for the $\{FeS_2His_2\}$ site).[13] A similar isomer shift has also been observed for the complex $(NEt_4)_2[Fe_2(SEt)_6]$ (δ = 0.70 mm/s), though the quadrupole splitting is somewhat larger for that complex containing Fe^{II} in tetrahedral thiolate environment (ΔE_Q = 3.25 mm/s).[16] An increase of temperature to 80 K and further to 210 K led to gradual emergence of another Mössbauer doublet for $(NEt_4)_4\mathbf{1}$ with δ = 0.69 mm/s and ΔE_Q = 1.56 mm/s (see SI). We assume that this feature originates from solid-state effects since upon subsequent cooling to 6 K the spectrum fully reverts to the initial one shown in Figure 4. A solution of diferrous $(NEt_4)_4\mathbf{1}$ was studied by Mössbauer spectroscopy as well. The sample was generated electrochemi-

dx.doi.org/10.1021/ja311563y | J. Am. Chem. Soc. 2013, 135, 1704–1707

cally via controlled potential coulometry (CPC) at −25 °C and −2.6 V versus Cp_2Fe/Cp_2Fe^+ in DMF/0.2 M $[NBu_4]PF_6$. The resulting Mössbauer spectrum was then recorded at 80 K and shows a major quadrupole doublet with δ = 0.78 mm/s and ΔE_Q = 2.71 mm/s (see SI), essentially identical to the solid state spectrum at 6 K. This confirms that the second doublet seen at elevated temperatures in the solid state spectrum, but absent in the frozen solution sample, is likely caused by solid state effects, and does not reflect intrinsic variations in the electronic structure of the molecular complexes.[17]

Because of the extreme sensitivity of $(NEt_4)_4$**1**, it was not possible to obtain sufficiently pure material for collecting SQUID data. Mössbauer spectroscopy in applied magnetic field at variable temperatures was thus performed to establish a lower limit for the magnetic exchange coupling−J, defined as $H = -2JS_A \cdot S_B$. Up to 40 K, the spectra show only weak magnetic splitting, virtually from the applied field only (Figure 5). The

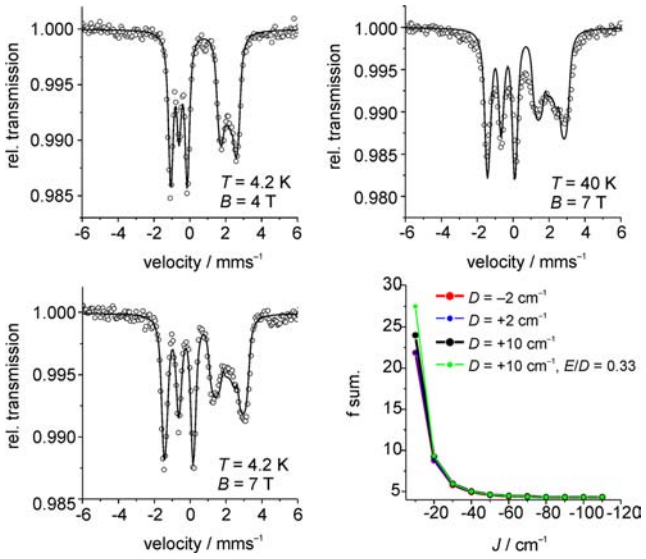

Figure 5. Magnetic field Mössbauer spectra of $(NEt_4)_4$**1** generated via CPC. The solid black lines are the result of a global spin Hamiltonian simulation for a dinuclear $S_A = S_B = 2$ system with δ = 0.78 mm/s, ΔE_Q = 2.74 mm/s, η = 0.35, D = +10 cm^{-1}, J = −30 cm^{-1} ($H = -2JS_A \cdot S_B$). Lower right: plot of the error sum of the simulations as a function of exchange coupling parameter J.

absence of significant internal fields (<0.1 T) evidences a rather well isolated diamagnetic S_T = 0 ground state without much level mixing or population of excited spin states. To establish an upper limit for the exchange coupling, J was varied in 10 cm^{-1} steps during iterative spin-Hamiltonian simulations with local spins S_{Fe} = 2, keeping the hyperfine tensors at a typical value $A_{Fe}/g_N\mu_N$ = −20 T and varying the zero field splitting parameter D in the range ±10 cm^{-1}. A plot of the resulting error sum of the simulations as a function of J is shown in the lower right part of Figure 5, revealing a flat minimum due to fading of the internal field for strong coupling. Taking into account inaccuracy and inhomogeneity of the applied field (ca. 0.1 T), we estimate $-J \geq 30$ cm^{-1} to be a safe assumption; a corresponding simulation is shown in Figure 5. This estimate for J is in good agreement with $-J \geq 40$ cm^{-1} derived from Mössbauer spectra of the Cr^{II}-treated *Aquifex aeolicus* ferredoxin.[12] Moreover, it shows that the antiferromagnetic coupling in $(NEt_4)_4$**1** may be consistent with the strong coupling measured for $(NEt_4)_2[Fe_2(SEt)_6]$ that also shows a planar $Fe(\mu\text{-}SR)_2Fe$ bridge between tetrahedral Fe^{II} sites.[16]

In summary we have, for the first time, isolated and crystallographically characterized a fully reduced diferrous [2Fe−2S] cluster with $Fe(\mu\text{-}S)_2Fe$ core. Thus, structural information is now available for a complete series of [2Fe−2S] model complexes $(NEt_4)_x[LFe(\mu\text{-}S)_2FeL]$ (x = 2, 3, 4) having the same bis(benzimidazolato) capping ligand L. Mössbauer studies on the new diferrous cluster show parameters very similar to the few data available for artificially super-reduced [2Fe−2S] proteins, and they provide a lower limit for the magnetic exchange coupling ($-J \geq 30$ cm^{-1}). The present results not only fill a blank spot in synthetic analogue Fe/S chemistry, but may also provide a valuable basis for identifying potential [2Fe−2S] cofactors that make use of their fully reduced diferrous state under physiological conditions. One should note that new Fe/S cluster types and Fe/S clusters with unusual redox couples and exciting biological functions continue to be discovered.[18]

■ ASSOCIATED CONTENT

Supporting Information

Synthetic procedures and complete experimental details; additional Mössbauer spectra; crystallographic details (CIF) for $(NEt_4)_3$**1** and $(NEt_4)_4$**1**. This material is available free of charge via the Internet at http://pubs.acs.org.

■ AUTHOR INFORMATION

Corresponding Author

franc.meyer@chemie.uni-goettingen.de

Notes

The authors declare no competing financial interest.

■ ACKNOWLEDGMENTS

Financial support by the DFG (International Research Training Group GRK 1422 "Metal Sites in Biomolecules: Structures, Regulation and Mechanisms"; see www.biometals.eu) and the Cusanuswerk (Ph.D. fellowship for A.A.) is gratefully acknowledged.

■ REFERENCES

(1) Beinert, H.; Holm, R. H.; Münck, E. *Science* **1997**, *277*, 653−659.
(2) Solomon, E. I.; Xie, X.; Dey, A. *Chem. Soc. Rev.* **2008**, *37*, 623−638.
(3) (a) Beinert, H. *J. Biol. Inorg. Chem.* **2000**, *5*, 2−15. (b) Carter, C. W., Jr. In *Handbook of Metalloproteins*; Messerschmidt, A., Ed.; 2001; Vol. *1*, pp 602−609.
(4) Rao, P. V.; Holm, R. H. *Chem. Rev.* **2004**, *104*, 527−559.
(5) Albers, A.; Demeshko, S.; Dechert, S.; Bill, E.; Bothe, E.; Meyer, F. *Angew. Chem.* **2011**, *123*, 9357−9361; *Angew. Chem., Int. Ed.* **2011**, *50*, 9191−9194.
(6) A second example has recently been published: Saouma, C. T.; Kaminsky, W.; Mayer, J. M. *J. Am. Chem. Soc.* **2012**, *134*, 7293−7296.
(7) (a) Watt, G. D.; Reddy, K. R. N. *J. Inorg. Biochem.* **1994**, *53*, 281−294. (b) Angove, H. C.; Yoo, S. J.; Burgess, B. K.; Münck, E. *J. Am. Chem. Soc.* **1997**, *119*, 8730−8731.
(8) Hans, M.; Buckel, W.; Bill, E. *J. Biol. Inorg. Chem.* **2008**, *13*, 563−579.
(9) Scott, T. A.; Berlinguette, C. P.; Holm, R. H.; Zhou, H.-C. *Proc. Natl. Acad. Sci. U.S.A.* **2005**, *102*, 9741−9744.
(10) (a) Deng, L.; Holm, R. H. *J. Am. Chem. Soc.* **2008**, *130*, 9878−9886. (b) Chakrabarti, M.; Deng, L.; Holm, R. H.; Münck, E.; Bominaar, E. L. *Inorg. Chem.* **2009**, *48*, 2735−2747.

(11) Im, S.-C.; Kohzuma, T.; McFarlane, W.; Gaillard, J.; Sykes, A. G. *Inorg. Chem.* **1997**, *36*, 1388−1396.
(12) Yoo, S. J.; Meyer, J.; Münck, E. *J. Am. Chem. Soc.* **1999**, *121*, 10450−10451.
(13) Leggate, E. J.; Bill, E.; Essigke, T.; Ullmann, G. M.; Hirst, J. *Proc. Natl. Acad. Sci. U.S.A.* **2004**, *101*, 10913−10918.
(14) Beardwood, P.; Gibson, J. F. *J. Chem. Soc., Dalton Trans.* **1992**, 2457−2466.
(15) Both $(NEt_4)_2$**1** and $(NEt_4)_3$**1** crystallize in the same space group $P\bar{1}$, while $(NEt_4)_4$**1** crystallizes in space group $C2/c$ and, therefore, has a mirror plane instead of an inversion center.
(16) Sanakis, Y.; Yoo, S. J.; Osterloh, F.; Holm, R. H.; Münck, E. *Inorg. Chem.* **2002**, *41*, 7081−7085.
(17) The cause of the second doublet emerging in the solid state spectrum is not known yet, but it might reflect an interesting phenomenon that will be studied in future work.
(18) (a) Bill, E. *Hyperfine Interact.* **2012**, *205*, 139−147. (b) Grubel, K.; Holland, P. L. *Angew. Chem., Int. Ed.* **2012**, *51*, 3308−3310.